

# From Single Molecule to Crystal: Mapping Out the Conformations of Tartaric Acids and Their Derivatives

Agnieszka Janiak, Urszula Rychlewska, Marcin Kwit, Urszula Stępień, Krystyna Gawrońska, and Jacek Gawroński\*<sup>[a]</sup>

Stereoisomers of one of the most important organic compounds, tartaric acid, optically active and *meso* as well as the ester or amide derivatives, can show diverse structures related to the rotation around the three carbon–carbon bonds. This study determines the controlling factors for conformational changes of these molecules in vacuo, in solution, and in the crystalline state using DFT calculations, spectroscopic measure-

ments, and X-ray diffraction. All structural variations can be logically accounted for by the possibility of formation and breaking of hydrogen bonds between the hydroxy or amide donors and oxygen acceptors, among these the hydrogen bonds that close five-membered rings being the most stable. These findings are useful in designing molecular and crystal structures of highly polar, polyfunctional, chiral compounds.

## 1. Introduction

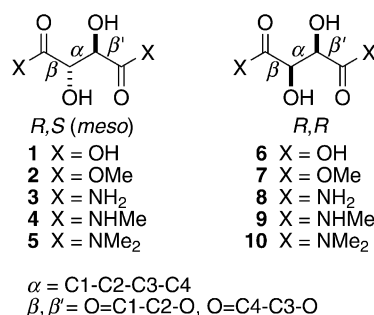
The fascinating history of optically active tartaric acid, one of the most important organic compounds existing in nature and rightfully called a “lab animal” for its chemical history, reflects numerous discoveries pertaining to the concepts of stereoisomerism and chirality by Pasteur and followers<sup>[1]</sup> and to practical applications in stereoselective synthetic organic chemistry.<sup>[2]</sup> Its optically inactive diastereoisomer, *meso*-tartaric acid, is not available from renewable resources, but nevertheless it has found uses in stereodifferentiating syntheses.<sup>[3]</sup>

Whereas the structure of natural (*R,R*)-tartaric acid has been the subject of several studies in the past, its conformation and the conformations of its derivatives remained a less known property. Even less is known about the structure of the *meso* stereoisomer, (*R,S*)-tartaric acid. The past studies included absolute configuration determination of natural tartaric acid by X-ray diffraction (Bijvoet, 1951),<sup>[4]</sup> and conformational studies using NMR spectroscopy, electronic circular dichroism (ECD), and vibrational circular dichroism (VCD), supplemented by ab initio calculations and X-ray diffraction analysis. Specifically, the studies involved natural tartaric acid derivatives,<sup>[5]</sup> dialkyl tartrates,<sup>[6]</sup> tartaronitriles,<sup>[7]</sup> and a dianion of tartaric acid.<sup>[8]</sup>

In this study we show that the structure of polar molecules such as tartaric acids and their derivatives is primarily controlled by the possibility to form multiple hydrogen bonds (HBs) under given conditions. The studies include DFT calculations for a single molecule, for a simulated continuous model of water solution (polarizable continuum model (PCM)), and X-ray determination of crystal structures of derivatives of *meso*-tartaric acid. The structure calculations were confronted with the results of conformational studies of tartaric acids and their

derivatives in polar solutions, using NMR and ECD spectra, where applicable. These studies are aimed at better understanding the structural changes the molecules undergo on a pathway from the isolated to the highly ordered crystal state.

The representative structures considered here include the acids, their esters, and amides **1–10**, shown in Scheme 1.



Scheme 1.

## 2. Results and Discussion

Tartaric acids and derivatives can (and in fact do) display numerous structures, due to configurational isomerism and con-

<sup>1</sup> It is pertinent to note that the year 2011 was marked as the 110th anniversary of the Nobel Prize in Physics, awarded to Wilhelm Röntgen, the discoverer of X-rays, and as the 110th anniversary of the first Nobel Prize in Chemistry, awarded to Jacobus H. van't Hoff, the discoverer of the laws of chemical dynamics and a pioneer in the field of stereochemistry.

[a] Dr. A. Janiak, Prof. Dr. U. Rychlewska, Dr. M. Kwit, U. Stępień, Dr. K. Gawrońska, Prof. Dr. J. Gawroński  
 Department of Chemistry  
 A. Mickiewicz University  
 Grunwaldzka 6, 60 780 Poznan (Poland)  
 Fax: (+ 48) 61-8291505  
 E-mail: gawronsk@amu.edu.pl

Supporting information for this article is available on the WWW under <http://dx.doi.org/10.1002/cphc.201200033>.

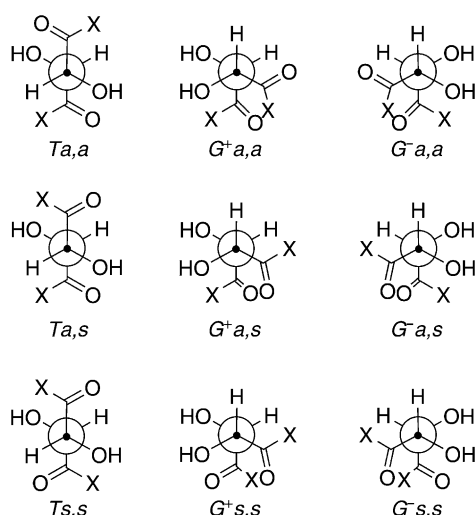


**Figure 1.** Conformational profile of (*R,S*)-tartaric acid derivatives. Conformers *Ta,a* and *Ts,s* are centrosymmetric and therefore achiral. *Ta,s* and its mirror image form a racemate. Conformers *G<sup>+</sup>a,a/G<sup>-</sup>a,a*, *G<sup>+</sup>a,s/G<sup>-</sup>a,s*, and *G<sup>+</sup>s,s/G<sup>-</sup>s,s* are enantiomers.

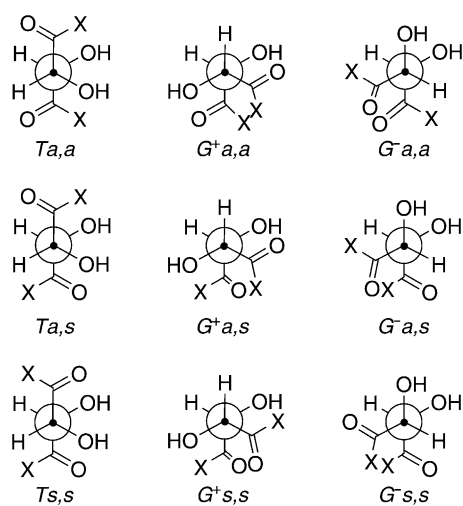


**Figure 2.** Conformational profile of (*R,R*)-tartaric acid derivatives. All conformers are chiral and have their mirror image counterparts in (*S,S*)-tartaric acid derivatives.

formational flexibility of the carbon chain. These are shown in Figure 1 and Figure 2.

Distinct conformers of 1–10 can be defined by torsion angles  $\alpha$ ,  $\beta$ , and  $\beta'$ , defined in Scheme 1. Figure 1 and Figure 2 represent generalized structures of molecules with either *trans* (*T*) or *gauche* (*G*) carbon chain and either *syn* (*s*) or *anti* (*a*) arrangement of vicinal C=O and C–O bonds. In the *R,S* series conformers *Ta,a* and *Ts,s* are of  $C_i$  symmetry and therefore achiral whereas *G* conformers are chiral ( $C_1$ ). Also chiral are all conformers in the *R,R* (or *S,S*) series and  $C_2$  symmetry is ascribed to *Ta,a*, *Ts,s*, *Ga,a*, and *Gs,s* structures.

Calculations for single molecules 1–10 were performed as described in the Experimental Section, first by generating a number of low-energy conformers with the use of molecular mechanics (MM3 force field) and CAChe WS Pro 5.0 software.<sup>[11]</sup> All the conformers found at the molecular mechanics level were pre-optimized with the use of the most popular B3LYP/6-31G(d) method<sup>[12]</sup> and then finally optimized at the M06-2X/Aug-cc-pVTZ level<sup>[13]</sup> (relative energies ( $\Delta E$  and  $\Delta G$ )

and percentage populations in vacuo are listed in Table 1). Additionally single-point energy calculations were performed at the B2PLYP(D)/Aug-cc-pVTZ level<sup>[14,15]</sup> (see Tables 1S and 2S in

**Table 1.** Conformer types of 1–10, stabilizing interactions (Figure 4), relative energies [ $\text{kcal mol}^{-1}$ ],<sup>[a]</sup> and percentage populations in vacuo calculated at the M06-2X/Aug-cc-pVTZ level and found in the solid state by X-ray diffraction.

Compound	Conformer type	Stabilizing interactions <sup>[b]</sup>	$\Delta E_{\text{vac}}$	Pop.	$\Delta G_{\text{vac}}$	Pop.	Conformer in crystals	Intramolecular stabilizing interactions
1	<i>Ta,a</i>	2(A+C)	0.00	77	0.00	61	<i>Gs,s</i> <sup>[c]</sup>	<b>K</b>
	<i>Ts,s</i>	2(B+E)	0.72	23	0.92	13	<i>Gs,s</i> <sup>[d]</sup>	not specified
	<i>Gs,s</i>	2B	–	–	0.92	26	<i>Ga,s</i> <sup>[d]</sup>	not specified
2	<i>Gs,s</i>	2B	0.00	70	0.00	68	<i>Gs,s</i> <sup>[e]</sup>	<b>B</b> <sup>[f]</sup>
	<i>Ga,s</i>	B + G	0.50	30	0.42	32		
3	<i>Ta,a</i>	2(A+D)	0.00	90	0.00	94	<i>Ga,a</i>	2D, J
	<i>Ts,s</i>	2(B+F)	1.33	10	1.62	6		
4	<i>Ta,a</i>	2(A+D)	0.00	96	0.00	83	<i>Ga,a</i>	2D, J
	<i>Ts,s</i>	2(B+F)	1.88	4	0.94	17		
5	<i>Ta,a</i>	2A	0.00	64	1.23	5	<i>Ts,s</i>	2B, <sup>[f]</sup> 2J
	<i>Ts,s</i>	2B	0.57	25	1.23	5		
	<i>Ga,p</i> <sup>[g]</sup>	A + G	1.67	8	0.00	90		
6	<i>G<sup>+</sup>a,a</i>	2(A+C)	0.00	64	1.27	10	<i>Ts,s</i> <sup>[h]</sup>	<b>G</b> <sup>[f]</sup> 2K
	<i>Ts,s</i>	2B	0.53	26	0.00	74		
	<i>G<sup>+</sup>s,s</i>	2(B+E)	1.38	6	–	–		
	<i>G<sup>+</sup>a,s</i>	A, A + C	1.60	4	–	–		
7	<i>Ta,s</i>	B + G and/or C, <sup>[g]</sup> J	–	–	1.02	16		
	<i>Ts,s</i>	2B	0.00	93	0.00	93	<i>Ta,s</i> <sup>[i]</sup>	<b>G, J, K</b>
	<i>Ta,s</i>	B, H, J	1.53	7	1.57	7		
8	<i>G<sup>+</sup>a,a</i>	2(A+D)	0.00	88	0.00	77	<i>Ta,a</i> <sup>[i]</sup>	2D, G, 2J
	<i>G<sup>-</sup>a,s</i>	B + G + D, I	1.50	7	1.01	14		
	<i>G<sup>+</sup>s,s</i>	2(B+F)	1.69	5	1.23	9		
9	<i>G<sup>+</sup>a,a</i>	2(A+D)	0.00	≈ 100	0.00	88	<i>Ta,a</i> <sup>[i]</sup>	2D, 2J
	<i>G<sup>-</sup>a,s</i>	2(B+F)	–	–	1.51	7		
	<i>G<sup>+</sup>s,s</i>	2D, G, 2J	–	–	1.76	5		
10	<i>G<sup>+</sup>s,s</i>	2B	0.00	87	0.00	66	<i>G<sup>-</sup>p,p</i> <sup>[j]</sup>	not specified
	<i>G<sup>+</sup>a,a</i>	2A	1.10	13	0.38	34		

[a] Conformers with relative energies above 2 kcal mol<sup>-1</sup> are not shown. [b] Interactions due to H...O distances longer than 2.55 Å are not listed. [c] Data from ref. [9]. [d] Hydrated forms. [e] Data from ref. [16]. [f] Component of a three-center HB. [g] Sum of conformers with C and/or G hydrogen-bond pattern. [h] Data from ref. [10]. [i] Data from ref. [5]. [j] In this conformer the angle  $\alpha$  (and  $\alpha'$ ) is close to 90°.

the Supporting Information; specific values of torsion angles for calculated individual conformers of **1–10** are given in Tables 3S and 4S, Supporting Information). The results turned out qualitatively similar in terms of conformer populations (see discussion below). Representative calculated types of conformers are shown in Figure 3 (see also the Supporting Information for a color version of Figure 3), while all low-energy conformers found by calculations are depicted in Figures 1S and 2S (Supporting Information). In addition, Table 1 includes structural characteristics of the conformers present in crystals, either determined for the present work (**3–5**) or taken from the literature for comparison (**1, 2, 6–10**). Selected torsion angles describing the molecular conformations found in crystals are listed in Table 2. We have also performed calculations of conformer populations in a medium simulating water. Due to intrinsic limitations of the PCM for water solution, the results are used only for confrontation with the experimental data (ECD, NMR) in water solution and are listed in Tables 1S and 2S (Supporting Information).

Our attempt to understand the logic of the conformational changes of tartaric acid derivatives due to the change of configuration and interaction with the medium starts with the analysis of results of structure calculations for individual conformers of single molecules. The results show that all low-energy conformers are stabilized by multiple HBs and 1,3-CH/CO dipole–dipole interactions; the possible types of these are shown in Figure 4.

In all structures **1–10** the hydroxy–carbonyl (**A, B**) and carboxy or amide–hydroxy (**C–F**) HBs are encountered (**B** type the most), often in cooperative pairs (**A+C, A+D, A+G; B+E, B+F, B+G; D+G**). In  $C_2$ - and  $C_2$ -symmetrical structures these pairs are doubled, which makes such structures particularly stable in the isolated molecules. Calculated H donor–oxygen acceptor distances vary within each type of HB (**A** 1.81–2.08, **B** 1.88–2.19, **C** 1.85–2.06, **D** 2.07–2.23 Å). In the overwhelming majority of the HB-forming six-membered rings **A** and **E**, the donor–acceptor distances are the shortest, below 2.0 Å. Short HBs (below 1.9 Å) are also observed in seven-membered-ring type **I** in tartramides **8** and **9**. Intramolecular hydroxy–hydroxy (**G**) and hydroxy–alkoxy (**H**) bonds are apparently weaker. In the case of **G** the donor–acceptor distance is within 2.3–2.5 Å, except in tartramides **8** and **9** (1.92–1.94 Å) where it is a part of a cooperative three-HB system. Except for **G**, all other types of intramolecular HBs directly affect the *syn*, *anti* conformation of the molecules; *anti* is obviously associated with **A, C, D**, and **H**, while **B, E, F**, and **I** are associated with the *syn* conformation of the vicinal C=O and C–O bonds. The presence of a **G**-type HB is associated with the preference for a *gauche* conformer in the *R,S* series and a *trans* conformer in the *R,R* series.

Intuitively one would expect a planar carbon chain conforma-

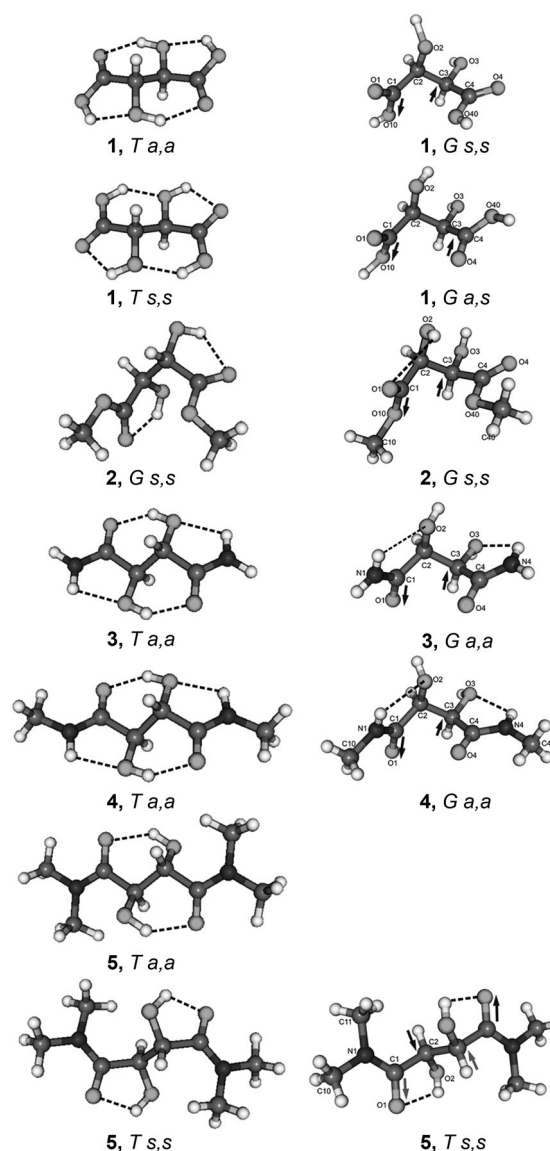


**Figure 3.** Calculated (left column) and X-ray diffraction determined (right column) structures of (*R,S*)-tartaric acid and its derivatives, with intramolecular HBs shown as broken lines and with arrows illustrating the antiparallel arrangement of local dipoles situated in 1,3-positions. HBs due to H...O distances longer than 2.55 Å are not shown. Labels mark the symmetry-independent part of molecules in crystals, the remaining part being generated by the symmetry transformation  $1-x, 2-y, 1-z$ . Data for X-ray determined structures of **1**<sup>[9]</sup> and **2**<sup>[10]</sup> are taken from the literature.

**Table 2.** Selected torsion angles [°] describing the molecular conformation in crystals of *meso*-tartaric acid, its ester and amides.<sup>[a]</sup>

Compound	Torsion angle			
	C1–C2–C3(C2)–C4(C1)	O2–C2–C3(C2)–O3(O2)	O1=C1–C2–O2	O4=C4–C3–O3
<b>1</b> <sup>[b]</sup>	–75.0(8)	–71.1(8)	–8.8(8)	11.7(8)
<b>1</b> × H <sub>2</sub> O <sub>(tridinic)</sub> <sup>[b]</sup>	–73.4(5)	–71.3(5)	–5.7(5)	–4.2(5)
<b>1</b> × H <sub>2</sub> O <sub>(monoclinic)</sub> <sup>[b]</sup>	–75.4(5)	–73.4(5)	173.3(5)	–7.0(5)
<b>2</b> <sup>[c]</sup>	–75.7(4)	–75.3(6)	0.2(5)	4.5(5)
<b>3</b>	–81.6(1)	–82.6(1)	–175.2(1)	–173.2(1)
<b>4</b>	–73.6(1)	–71.9(1)	–173.4(1)	166.0(1)
<b>5</b>	180	180	37.3(2)	37.3(2)

[a] Derivatives crystallizing in the *gauche* conformation are presented consistently as *G*<sup>–</sup> enantiomers, with literature data adapted accordingly. [b] Data from ref. [9]. [c] Data from ref. [10].

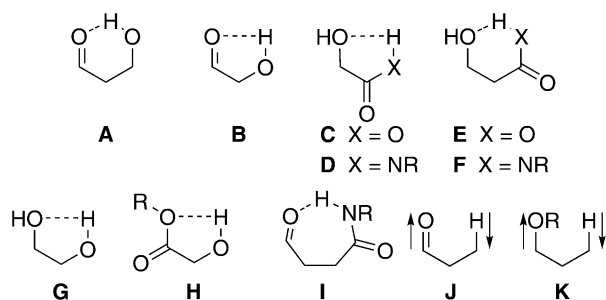


**Figure 4.** Possible stabilizing intramolecular interactions in tartaric acids and their derivatives. Dashed lines indicate HBs while arrows in J and K mark antiparallel local dipoles.

tion for a molecule with two adjacent chiral centers of opposite configuration, that is, in *meso*-tartaric acid. Indeed, calculations carried out for **1** show a strong preference for *Ta,a* and *Ts,s* conformers of isolated molecules. These conformers are highly populated (jointly up to 100%, Table 1) due to the stabilizing action of cooperative intramolecular HBs involving the carboxy and hydroxy groups (2(A+C) in *Ta,a* or 2(B+E) in *Ts,s*). *Gauche* conformers of *meso*-tartaric acid may contribute more significantly to the equilibrium in a medium of higher polarity such as water. This is apparently due to limited possibilities to form intramolecular HBs in a bent carbon atom skeleton of **1**: in *gauche* conformers the carboxylic groups are not involved in intramolecular hydrogen bonding, according to calculations. Experimentally this is supported by the fact that the  $^3J_{\text{H,H}}$  coupling constant in the  $^1\text{H}$  NMR spectrum of **1** measured in  $\text{D}_2\text{O}$  solution is low, typical for the *gauche* conformer. In the crystal structure of **1**<sup>[9]</sup> the *Gs,s* conformer is indeed present, in which the carboxylic groups are solely involved in intermolecular HBs, either with themselves or with water molecules as mediators.

In the case of diastereomeric natural tartaric acid (**6**) the preferred conformation of the isolated molecule is  $G^+a,a$  (in  $\Delta E$ ), just opposite to that of **1**. This conformer is stabilized by cooperative HBs 2(A+C) and similarly other bent conformers  $G^+s,s$ , 2(B+E), and  $G^+a,s$  (A, A+C) are stabilized. *Trans* conformers are less populated: the *Ts,s* population is one third that of *gauche* conformers, since *trans* conformers are not stabilized by cooperative HBs. However, in polar environments the proportion of *trans* conformers increases and the presence of *trans* conformers is again supported by a low  $^3J_{\text{H,H}}$  coupling constant (2.4 Hz) of **6** in the  $^1\text{H}$  NMR spectrum in  $\text{D}_2\text{O}$  solution. In the crystal structure of **6** the *Ts,s* conformer is present.<sup>[16]</sup> In this structure the intramolecular HB of the G type (Figure 4) appears as a minor component of a three-center bond (the other component being intermolecular) and the intramolecular bond of the B type is replaced by the so-called mediated HB.<sup>[17]</sup>

The number of HB donors is significantly reduced in the diester derivative **2**, and therefore cooperative HBs stabilizing *trans* conformers are not available. According to calculations, *gauche* conformers constituting the minority in the case of diacid **1** are dominant in the case of diester **2**. Among these, conformer *Gs,s* stabilized by two B-type HBs is the most popu-

lated (70%). The distribution of conformers is not much different in water medium and the presence of *gauche* conformers is confirmed by a low  $^3J_{\text{H,H}}$  coupling constant (2.7 Hz) in  $\text{D}_2\text{O}$  solution. Furthermore, the *Gs,s* conformation is preserved in the crystal structure<sup>[10]</sup> where only one of the two possible intramolecular HBs of the B type is preserved but in a diminishing form, that is, as a minor component of the three-center bond with other components being intermolecular. The remarkable stability of the conformation of diester **2** is apparently due to a lack of HBs that can be broken by intermolecular interactions.

Diastereomer **7**, as expected, is exclusively in a *trans* conformation, with the *Ts,s* conformer stabilized by two B-type HBs having the lowest energy as a single molecule (93%). This type of conformational preference in solution is supported by measured low values of the  $^3J_{\text{H,H}}$  coupling constant of **7** in polar solvents. Further support for the *syn* conformation in the most abundant *Ts,s* conformer comes from ECD measurements in water solution,<sup>[5]</sup> and recently this conformer was determined as the lowest-energy component of the equilibrium in nonpolar solvent by VCD measurements.<sup>[6]</sup> It was found that polar solvent (DMSO) favors formation of intermolecular hydrogen-bonded clusters between **7** and DMSO.<sup>[6]</sup> In the crystal the preferred structure of **7** is *Ta,s*.<sup>[5]</sup> The B-type intramolecular HBs no longer stabilize the extended conformation but instead, the G-type HB appears as a minor component of a three-center bond, the other component being intermolecular.

Primary and secondary diamides **3** and **4** behave similarly in computational structural studies. The planar amide structure combined with strong acceptor properties of the amide C=O group (due to polarization of the amide group) and HB donor properties of the amine hydrogen atom(s) make the number of available structures for these molecules very limited. In fact, the preferred conformers of diamides are similar to those of diacid **1**, that is, *Ta,a* and *Ts,s*, where there are cooperative intramolecular HBs involving the C=O, OH, and NH groups 2(A+D) in *Ta,a* (over 84% in equilibrium) or 2(B+E) in *Ts,s*. On the other hand, the preferred *gauche* conformation of diamides **3** and **4** in polar solutions (DMSO and  $\text{D}_2\text{O}$ ) receives strong experimental support from the low measured values of  $^3J_{\text{H,H}}$  coupling constants (3.2 and 2.6 Hz for **3**, 3.3 Hz for **4**). It should be noted that the calculations of conformer population in simulated (PCM) water solution for highly polar diamide molecules do not accurately represent the actual conformer population in water solutions, as these calculations neglect intermolecular interactions with explicit water molecules. Low-energy *gauche* conformers of NH diamides in water solutions do not possess the two cooperative HBs present in *trans* conformers. For example, the *Ga,s* conformer is stabilized by one cooperative D+G+B HB system and one unusual, I-type, seven-membered HB ring, joining the NH donor of one amide group with the C=O acceptor of the other amide group. Other *gauche* conformers would leave NH donors and/or C=O acceptors available for intermolecular hydrogen bonding, for example with the solvent molecules. The structure of diamides **3** and **4** in the crystal is therefore *Ga,a* since in this conformer the only intramolecular HBs utilized are two of D type

(Figure 3), which allows the various types of intermolecular HBs to be formed (intermolecular interactions will be discussed in a separate paper).

The tartramides of natural configuration **8** and **9** do not differ in their conformational profile; however, their calculated low-energy conformers are different from those of diastereomeric diamides **3** and **4**. The lowest-energy conformers of **8** and **9** are (+)-*gauche*,  $G^+a,a$  dominating (over 88%). This conformer was found to be the most stable by previous calculations at the HF/6-31G level.<sup>[5]</sup> In *gauche* conformers the stabilizing factors are the same as in the case of low-energy conformers of **3** and **4**, that is, two **A** + **D**-type HBs in  $G^+a,a$  conformers and two **B** + **E**-type HBs in  $G^+s,s$  conformers. A small contribution of another conformer,  $G^-a,s$ , stabilized by one cooperative **D** + **G** + **B** and one **I**-type HB system, is calculated for isolated molecule **8**. Whereas calculations for simulated water solution yield a conformer distribution similar to that for the isolated molecule, the experimental evidence gathered earlier (<sup>1</sup>H NMR, ECD)<sup>[5]</sup> strongly supports a *Ta,a* conformer of **8** or **9** as a dominant one in water solutions. In this conformer available intramolecular HBs are of **D** type, thus leaving other oxygen donors and acceptors accessible for intermolecular hydrogen bonding. Consequently, in the crystal the conformation of diamides **8** and **9** is *Ta,a*.<sup>[5]</sup>

Tetraalkylated diamide **5** represents a special case. *N,N*-Di-alkylation not only removes a strong NH donor but also it may introduce steric crowding, absent in other tartaric acid derivatives. As in the case of tartrate **2**, no cooperative intramolecular HBs are possible in **5**. Low-energy conformers of **5** are *trans* (over 80%) and are stabilized by two HBs, either type **A** (*Ta,a*) or **B** (*Ts,s*), the former prevailing for the isolated molecule. Despite its tertiary nature, the amide bond remains nearly planar in these two conformers and no steric crowding is apparent. <sup>1</sup>H NMR data indicate that in solution the *trans* conformation of **5** is preferred, which results in a higher value of the <sup>3</sup>*J*<sub>H,H</sub> coupling constant (7.3 Hz in CDCl<sub>3</sub>, 8.2 Hz in D<sub>2</sub>O). Significantly, the *Ts,s* conformer is just the one found in the crystal. It is stabilized by a pair of intramolecular HBs of the **B** type and again this intramolecular linkage is a part of the three-center HB with the other component intermolecular. Unlike in the previous cases, in this instance the intramolecular HB is quite strong and weakens the intermolecular component which consequently displays the longest donor–acceptor distances in the studied series.

A contribution from a higher-energy conformer of **5**, *Ga,p*, has been found by calculation. This conformer is of nontypical structure since one of the carbonyl groups and the vicinal C–O bond form a torsion angle close to 90° (*p*). Such a structural feature becomes dominant in the case of diastereomeric molecule **10** in the solid state. Here a *trans* conformation introduces significant crowding of the substituents, whereas steric crowding due to dialkylamino substituents is absent in the case of conformers (+)-*gauche*, according to calculations. As in the case of **5**, only two **B**-type (conformer  $G^+s,s$ ) or **A**-type (conformer  $G^+a,a$ ) intramolecular HBs stabilize the low-energy conformers of **10**. Conformer (+)-*gauche* are the lowest-energy structures calculated for molecules in vacuo. The experimental

<sup>3</sup>*J*<sub>H,H</sub> coupling constant of 2.9 Hz measured for **10** in CDCl<sub>3</sub> solution is in agreement with the dominant presence of the (+)-*gauche* conformers. However, in polar solvents (water, methanol) a much larger value (7.6 Hz) of the <sup>3</sup>*J*<sub>H,H</sub> coupling constant indicates that the preferred conformation is the one with vicinal hydrogen atoms *anti*, that is,  $G^-$ .<sup>[5]</sup> This has been confirmed by calculations with the use of the AMSOL method.<sup>[18]</sup> Interestingly, in the crystal diamide **10** assumes a rather unusual  $G^-p,p$  conformation in which the two vicinal O=C/C–O bonds are perpendicular and no intramolecular HB is present.<sup>[19]</sup> Therefore it is justified to say that *N,N*-tetraalkylated tartramides prefer a (+)-*gauche* conformation in nonpolar medium, stabilized by two intramolecular HBs, whereas in polar medium and in the crystal their conformation changes to (–)-*gauche*, which cannot be stabilized by strong intramolecular HBs but favors formation of very strong intermolecular HBs.<sup>[19]</sup>

Moreover, in all types of conformers present in crystals, there appears at least one pair of antiparallel CH and CO dipoles situated in the 1,3-positions.<sup>[20]</sup> The presence of such dipoles brings about an additional stabilizing effect, **J** and **K**, although apparently less significant than hydrogen bonding. In molecules possessing the *trans* conformation the effect is doubled (Figure 3).

In general, the available data and the discussion above indicate reshuffling of the conformer population on going from molecules in vacuo to polar solution and to crystal, but only in the case of polar diacids **1** (*T*→*G*) and **6** ( $G^+$ →*T*) and NH-diamides **3**, **4** (*T*→*G*), **8**, and **9** ( $G^+$ →*T*). The conformations of less polar derivatives, diesters and tetraalkyldiamides are less dramatically affected by the molecular environment and remain *G* for **2**, *T* for **5**, and **7** and  $G^+/G^-$  for **10**. Note that in all cases the diastereoisomeric tartaric acid derivatives assume the opposite preferred conformation, *G* or *T*.

### 3. Conclusions

Despite a large number of variables that should be considered, the conformation of tartaric acids and their derivatives under various external conditions (molecules in vacuo, in water, and in the crystal) could be readily determined with the use of molecular modeling, NMR and ECD spectra, and X-ray diffraction analysis. The results obtained are complementary and consistent for both the *R,S* and the natural *R,R* series; the data for the latter series<sup>[5]</sup> were used for comparison. Therefore, for the first time we are in a position to correlate conformational changes caused by a change of relative configuration *R,S/R,R*, molecule substitution, and molecule environment (in vacuo/in the crystal). The results are summarized in Figure 5.

The results of Figure 5 and Table 1 can be interpreted in terms of available number and relative stability of intramolecular HBs. Molecules of lower polarity (diesters **2**, **7** or tetraalkyldiamides **5**, **10**) do not change the preferred conformation (*trans* or *gauche*) on going from a single molecule to the crystal. The opposite holds for polar diacids **1** and **6** and diamides **3**, **4**, **8**, and **9**. This is because intermolecular interactions (polar environment, crystal formation) weaken HBs of type **A**, **C**, and

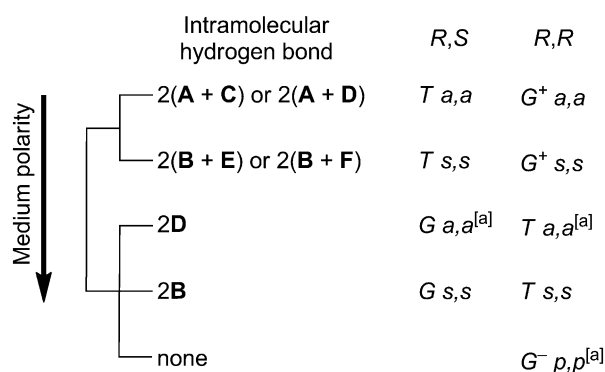


**Figure 5.** Summary of the hydrogen-bonding effect on conformational preferences of tartaric acid derivatives in media of increasing ability to form intermolecular HBs. [a] In the crystal.

E–H whereas the stronger HBs of type B and D are retained. Also retained is the antiparallel arrangement of at least one pair of local CH and CO dipoles (J or K), which imposes additional constraints on the spatial orientation of the two interacting bonds and therefore has an effect on the molecular conformation. In this way the molecular conformation is accordingly changed, although in crystals additional factors such as steric crowding may affect the conformation and make the less typical one (e.g. *G<sup>-</sup>p,p* in the crystal structure of **10**<sup>[19]</sup>) better suited for the crystal packing.

Tartaric acid and its derivatives are widely used not only for synthetic purposes but also for pharmaceutical formulations. The results presented here can be useful in designing molecular and crystal structures not only of tartaric acid derivatives but also of other similar polyfunctional compounds.

## Experimental Section

**Synthesis:** (*R,S*)-Tartaric acid diamides **3–5** were obtained from diester **2** by aminolysis with ammonia, methylamine, or dimethylamine in methanol solution at 5 °C for 1 week, according to a procedure described for aminolysis of diester **7**.<sup>[5]</sup> Crude products were purified by crystallization.

**meso-Tartramide (3):** M.p. 181–184 °C (methanol/water); <sup>1</sup>H NMR ([D<sub>6</sub>]DMSO): δ = 4.05 (d, *J* = 5.5 Hz, 2H), 5.59 (d, *J* = 5.5 Hz, 2H), 6.97 (s, 2H), 7.10 ppm (s, 2H); <sup>13</sup>C NMR ([D<sub>6</sub>]DMSO): δ = 72.7, 173.0 ppm; ESI(–) MS: *m/z* 147 (*M*–H); ESI(+) MS: *m/z* 171 (*M*+Na).

**meso-*N,N'*-Dimethyltartramide (4):** M.p. 181–184 °C (ethanol); <sup>1</sup>H NMR ([D<sub>6</sub>]DMSO): δ = 2.57 (d, *J* = 4.8 Hz, 6H), 4.10 (s, 2H), 5.75 (s, 2H), 7.53 ppm (q, *J* = 4.8 Hz, 2H); <sup>13</sup>C NMR ([D<sub>6</sub>]DMSO): δ = 25.3, 73.9, 171.3 ppm; ESI(–) MS: *m/z* 175 (*M*–H), ESI(+) MS *m/z* 199 (*M*+Na).

**meso-*N,N,N',N'*-Tetramethyltartramide (5):** M.p. 189–190 °C (chloroform/hexane); <sup>1</sup>H NMR (CDCl<sub>3</sub>): δ = 3.04 (s, 6H), 3.14 (s, 6H), 4.50 ppm (s, 2H); <sup>13</sup>C NMR (CDCl<sub>3</sub>): δ = 36.7, 70.4, 172.3 ppm; ESI(+) MS: *m/z* 227 (*M*+Na).

**X-ray Crystallography:** Reflection intensities for crystals of **3**, **4**, and **5** were measured on a SuperNova diffractometer equipped with a Cu microfocus source ( $\lambda = 1.54178$  Å) and 135 mm Atlas CCD de-

tektor at 290.0(1) K. Data reduction and analysis for these structures were carried out with CrysAlisPro program v.171.33.34d.<sup>[21]</sup> Multiscan correction for absorption was also applied.<sup>[22]</sup> All structures were solved by direct methods using SHELXS97,<sup>[23]</sup> and refined by the full-matrix least-squares technique with SHELXL97.<sup>[23]</sup> All heavy atoms were refined anisotropically. H atoms attached to N and O atoms were located reliably on difference Fourier maps and their positions and isotropic displacement parameters were refined. The methyl H atoms were first found in difference Fourier maps and then were allowed to rotate freely during refinement using the AFIX 137 command with C–H = 0.96 Å and  $U_{iso} = 1.5 U_{eq}(C)$ . The methine H atoms were placed in their idealized positions and were refined as riding on their parent atoms, with C–H distances of 0.98 Å and their  $U_{iso}$  values of 1.2  $U_{eq}(C)$ . In **3** all H atoms were located in a difference Fourier map and their positions and displacement parameters were refined freely. The rotational disorder in methyl groups of **4** and **5** was modeled as two equivalent 0.50 occupancies of H atoms.

Crystallographic data for **3–5** are presented in Table 7S (Supporting Information). Newman projections illustrating molecular conformations present in crystals of **1–5** are shown in Figure 3S (Supporting Information). CCDC-862696 (**3**), 862697 (**4**), and 862698 (**5**) contain the supplementary crystallographic data for this paper. These data can be obtained free of charge from The Cambridge Crystallographic Data Centre via [www.ccdc.cam.ac.uk/data\\_request/cif](http://www.ccdc.cam.ac.uk/data_request/cif).

**Computational Methods:** A preliminary conformer distribution search was performed by CONFLEX software (a part of the CAChe WS Pro package<sup>[11]</sup>) using the MM3 molecular mechanics force field. The systematic search of all possible conformers was performed using a molecular mechanics method taking into account all degrees of freedom of the molecule. The real minimum-energy conformers found by molecular mechanics were further fully optimized at the DFT/B3LYP/6-31G(d) level as implemented in the Gaussian 09 package.<sup>[24]</sup> This reduced significantly the number of conformers. Then all stable conformers, regardless of their relative energies, were reoptimized at the M06-2X/Aug-cc-pVTZ level<sup>[13]</sup> in vacuo and with the use of the PCM solvent model simulating water solution.<sup>[25]</sup> Conformers obtained at this stage were the real minima (no imaginary frequencies were found). To verify the results obtained with the use of the M06-2X functional, we performed single-point energy calculations with a new functional recently proposed by Grimme,<sup>[14]</sup> dubbed B2PLYP, which belongs to a general class of double-hybrid density functionals (DHDFs). Several studies have shown that DHDFs give very accurate results for large molecules, with energetic and thermodynamic data and molecular structures comparable to those obtained with the use of CCSD(T).<sup>[15]</sup> The calculations with the use of the B2PLYP(D) functional and Aug-cc-pVTZ basis set were performed for all structures optimized in the gas phase and with the use of the PCM solvent model.

The total energy values calculated at both M06-2X/Aug-cc-pVTZ and B2PLYP(D)/Aug-cc-pVTZ levels were used to obtain the Boltzmann population of conformers at 298.15 K. Only the results for conformers that differ from the most stable one by less than 2 kcal mol<sup>-1</sup> were taken into account for further calculations, following a generally accepted protocol.<sup>[26]</sup> Since the values of relative  $\Delta E$  energies and populations of the respective conformers obtained with the use of the B2PLYP(D)/Aug-cc-pVTZ method were not much different from those obtained with the use of the M06-2X/Aug-cc-pVTZ method, only the latter  $\Delta E$ -based data were taken into consideration and discussed here.

## Acknowledgements

A.J. thanks the Foundation for Polish Science for a FOCUS fellowship. All calculations were performed at the Poznań Supercomputing and Networking Center.

**Keywords:** density functional calculations • hydrogen bonds • structure elucidation • tartaric acid • X-ray crystallography

- [1] a) L. Pasteur in *The Foundations of Stereochemistry* (Ed.: G. M. Richardson), American Book Co., New York, **1901**, pp. 1–33; b) Z. S. Derewenda, *Acta Crystallogr. Sect. A* **2008**, *64*, 246–258.
- [2] a) J. Gawronski, K. Gawronska, *Tartaric and Malic Acids in Synthesis: A Source Book of Building Blocks, Ligands, Auxiliaries, and Resolving Agents*, Wiley, New York, **1999**; b) A. K. Ghosh, E. S. Koltun, G. Bilcer, *Synthesis* **2001**, 1281–1301.
- [3] a) K. H. Bell, *Aust. J. Chem.* **1987**, *40*, 399–404; b) H. J. Bestmann, U. C. Philipp, *Angew. Chem.* **1991**, *103*, 78–79; *Angew. Chem. Int. Ed. Engl.* **1991**, *30*, 86–88; c) M. Mikołajczyk, M. Mikina, M. W. Wiczorek, J. Błaszczak, *Angew. Chem.* **1996**, *108*, 1645–1647; *Angew. Chem. Int. Ed. Engl.* **1996**, *35*, 1560–1562.
- [4] A. F. Peerdman, A. J. van Bommel, J. M. Bijvoet, *Nature* **1951**, *168*, 271–272.
- [5] a) J. Gawronski, K. Gawronska, P. Skowronek, U. Rychlewska, B. Warzajtis, J. Rychlewski, M. Hoffmann, A. Szarecka, *Tetrahedron* **1997**, *53*, 6113–6144; b) J. Gawronski, K. Gawronska, U. Rychlewska, *Tetrahedron Lett.* **1989**, *30*, 6071–6074.
- [6] P. Zhang, P. L. Polavarapu, *J. Phys. Chem. A* **2007**, *111*, 858–871.
- [7] J. Gawronski, K. Gawronska, N. Wascinska, A. Plutecka, U. Rychlewska, *Polish J. Chem.* **2007**, *81*, 1917–1925.
- [8] M. Hoffmann, J. Grajewski, J. Gawronski, *New J. Chem.* **2010**, *34*, 2020–2026.
- [9] G. A. Bootsma, J. C. Schoone, *Acta Crystallogr.* **1967**, *22*, 522–532.
- [10] J. Kroon, J. A. Kanters, *Acta Crystallogr. Sect. B* **1973**, *29*, 1278–1283.
- [11] CAChe WS Pro 5.0, Fujitsu Ltd.
- [12] Y. Zhao, D. G. Truhlar, *Acc. Chem. Res.* **2008**, *41*, 157–167.
- [13] Y. Zhao, D. G. Truhlar, *Theor. Chem. Acc.* **2008**, *120*, 215–241.
- [14] S. J. Grimme, *J. Chem. Phys.* **2006**, *124*, 034108–034116.
- [15] a) F. Neese, T. Schwabe, S. Grimme, *J. Chem. Phys.* **2007**, *126*, 124115; b) T. Schwabe, S. Grimme, *Phys. Chem. Chem. Phys.* **2007**, *9*, 3397–3406.
- [16] Q.-B. Song, M.-Y. Teng, Y. Dong, C.-A. Ma, J. Sun, *Acta Crystallogr. Sect. E* **2006**, *62*, o33378–o33379.
- [17] U. Rychlewska, A. Szarecka, J. Rychlewski, R. Motała, *Acta Crystallogr. Sect. B* **1999**, *55*, 617–625.
- [18] a) A. Szarecka, J. Rychlewski, U. Rychlewska in *Quantum Systems in Chemistry and Physics, Vol. 2* (Eds.: A. Hernández-Laguna, J. Maruani, R. McWeeny, S. Wilson), Kluwer Academic Publishers, Dordrecht, **2000**, pp. 355–366; b) M. Hoffmann, J. Rychlewski, U. Rychlewska in *Computational Methods in Science and Technology, Vol. 2* (Eds.: J. Rychlewski, J. Węglarz, K. W. Wojciechowski), Scientific Publishers OWN, Poznań, **1996**, pp. 51–63; c) M. Hoffmann, A. Szarecka, J. Rychlewski, *Adv. Quantum Chem.* **1998**, *32*, 109–125; d) M. Hoffmann, J. Rychlewski in *New Trends in Quantum Systems in Chemistry and Physics, Vol. 2, Part VIII* (Eds.: J. Maruani, Ch. Minot, R. McWeeny, Y. G. Smeyers, S. Wilson), Kluwer Academic Publishers, Dordrecht, **1999**, pp. 189–210.
- [19] U. Rychlewska, *Acta Crystallogr. Sect. C* **1992**, *48*, 965–969.
- [20] J. Gawroński, A. Długocińska, J. Grajewski, A. Plutecka, U. Rychlewska, *Chirality* **2005**, *17*, 388–395.
- [21] CrysAlisPro, Version 1.171.33.34d, Oxford Diffraction Ltd., Yarnton, England, **2009**.
- [22] CrysAlis Software package, Scale3 abspack, Oxford Diffraction Ltd., Yarnton, England, **2006**.
- [23] G. M. Sheldrick, *Acta Crystallogr. Sect. A* **2008**, *64*, 112–120.
- [24] Gaussian 09 (Revision A.2), M. J. Frisch, G. W. Trucks, H. B. Schlegel, G. E. Scuseria, M. A. Robb, J. R. Cheeseman, G. Scalmani, V. Barone, B. Mennucci, G. A. Petersson, H. Nakatsuji, M. Caricato, X. Li, H. P. Hratchian, A. F. Izmaylov, J. Bloino, G. Zheng, J. L. Sonnenberg, M. Hada, M. Ehara, K. Toyota, R. Fukuda, J. Hasegawa, M. Ishida, T. Nakajima, Y. Honda, O. Kitao, H. Nakai, T. Vreven, J. A. Montgomery, Jr., J. E. Peralta, F. Ogliaro, M. Bearpark, J. J. Heyd, E. Brothers, K. N. Kudin, V. N. Staroverov, R. Kobayashi, J. Normand, K. Raghavachari, A. Rendell, J. C. Burant, S. S. Iyengar, J. Tomasi, M. Cossi, N. Rega, J. M. Millam, M. Klene, J. E. Knox, J. B. Cross, V. Bakken, C. Adamo, J. Jaramillo, R. Gomperts, R. E. Stratmann, O. Yazyev, A. J. Austin, R. Cammi, C. Pomelli, J. W. Ochterski, R. L. Martin, K. Morokuma, V. G. Zakrzewski, G. A. Voth, P. Salvador, J. J. Dannenberg, S. Dapprich, A. D. Daniels, Ö. Farkas, J. B. Foresman, J. V. Ortiz, J. Cioslowski, D. J. Fox, Gaussian, Inc., Wallingford, CT, **2009**.
- [25] J. Tomasi, B. Mennucci, R. Cammi, *Chem. Rev.* **2005**, *105*, 2999–3093.
- [26] a) P. J. Stephens, F. J. Devlin, J. R. Cheeseman, M. J. Frisch, O. Bortolini, P. Besse, *Chirality* **2003**, *15*, S57–S64; b) P. J. Stephens, D. M. McCann, E. Butkus, S. Stončius, J. R. Cheeseman, M. J. Frisch, *J. Org. Chem.* **2004**, *69*, 1948–1958; c) P. J. Stephens, D. M. McCann, F. J. Devlin, J. R. Cheeseman, M. J. Frisch, *J. Am. Chem. Soc.* **2004**, *126*, 7514–7521; d) P. J. Stephens, D. M. McCann, F. J. Devlin, A. B. Smith III, *J. Nat. Prod.* **2006**, *69*, 1055–1064.

Received: January 13, 2012

Published online on March 13, 2012